



Indocyanine Green-Loaded PLGA Nanoparticles Conjugated with Hyaluronic Acid Improve Target Specificity in Cervical Cancer Tumors

Seonmin Choi^{1*}, San-Hui Lee^{2*}, Sanghyo Park¹, Sun Hwa Park², Chaewon Park¹, and Jaehong Key¹

¹Department of Biomedical Engineering, Yonsei University, Wonju;

²Department of Obstetrics and Gynecology, Yonsei University Wonju College of Medicine, Wonju, Korea.

Purpose: Indocyanine green (ICG) is a promising agent for intraoperative visualization of tumor tissues and sentinel lymph nodes in early-stage gynecological cancer. However, it has some limitations, including a short half-life and poor solubility in aqueous solutions. This study aimed to enhance the efficacy of near-infrared (NIR) fluorescence imaging by overcoming the shortcomings of ICG using a nano-drug delivery system and improve target specificity in cervical cancer.

Materials and Methods: ICG and poly(lactic-co-glycolic acid) (PLGA) conjugated with polyethylenimine (PEI) were assembled to enhance stability. Hyaluronic acid (HA) was coated on PEI-PLGA-ICG nanoparticles to target CD44-positive cancer cells. The manufactured HA-ICG-PLGA nanoparticles (HINPs) were evaluated in vitro and in vivo on cervical cancer cells (SiHa; CD44+) and human dermal cells (ccd986sk; CD44-), respectively, using NIR imaging to compare intracellular uptake and to quantify the fluorescence intensities of cells and tumors.

Results: HINPs were confirmed to have a mean size of 200 nm and a zeta-potential of 33 mV using dynamic light scattering. The stability of the HINPs was confirmed at pH 5.0–8.0. Cytotoxicity assays, intracellular uptake assays, and cervical cancer xenograft models revealed that, compared to free ICG, the HINPs had significantly higher internalization by cervical cancer cells than normal cells ($p < 0.001$) and significantly higher accumulation in tumors ($p < 0.001$) via CD44 receptor-mediated endocytosis.

Conclusion: This study demonstrated the successful application of HINPs as nanocarriers for delivering ICG to CD44-positive cervical cancer, with improved efficacy in NIR fluorescence imaging.

Key Words: Fluorescence imaging, nanoparticles, cervix, indocyanine green, tumor targeting, cervical cancer

INTRODUCTION

Cervical cancer is the fourth leading cause of cancer related death in women worldwide, with an estimated 63604127 new cases and 341831 new deaths annually. Cervical cancer has be-

come a very serious problem, especially in developing countries, with incidence and mortality rates accounting for large proportions of the global cancer rate.¹⁻⁴

The most effective way to treat early-stage cervical cancer is to remove tumors via surgery. The goal of surgical treatment for malignant tumors is a complete disease-free margin. The introduction of imaging techniques that provide real-time information on metastasis and invasion during surgery has been found to facilitate the complete resection of tumors and the execution of additional surgery to assess metastasis. Fluorescence-based image-guided surgery is one surgical method that uses near-infrared (NIR) imaging in the wavelength range of 700–900 nm to provide real-time visualization and to improve the surgical removal of diseased areas. Among the various contrast media suitable for this wavelength range, indocyanine green (ICG), an FDA-approved NIR fluorescent dye,

Received: June 11, 2021 **Revised:** August 17, 2021

Accepted: August 23, 2021

Corresponding author: Jaehong Key, PhD, Department of Biomedical Engineering, Yonsei University, 1 Yonseidae-gil, Wonju 26493, Korea.
Tel: 82-33-760-2857, Fax: 82-33-760-2857, E-mail: jkey@yonsei.ac.kr

*Seonmin Choi and San-Hui Lee contributed equally to this work.

•The authors have no potential conflicts of interest to disclose.

© Copyright: Yonsei University College of Medicine 2021

This is an Open Access article distributed under the terms of the Creative Commons Attribution Non-Commercial License (<https://creativecommons.org/licenses/by-nc/4.0>) which permits unrestricted non-commercial use, distribution, and reproduction in any medium, provided the original work is properly cited.

is widely used clinically to map sentinel lymph nodes: studies on ICG NIR fluorescence in sentinel lymph nodes have been conducted in ovarian, gastric, rectal, breast, cervical, and endometrial cancers.⁵⁻⁸ However, ICG has a few drawbacks, including concentration-dependent aggregation,^{9,10} quenching due to aggregates,¹¹ poor solubility in aqueous solutions, easy chemical degradation due to exposure to light or temperature,¹² low target specificity, and a short half-life due to rapid clearance.¹³ These limitations make it difficult to detect the microscopic or regional metastatic spread of tumors, thus increasing the recurrence rate of cancers. Meanwhile, research has indicated that nanoparticles incorporating ICG could potentially overcome these shortcomings and be used as ideal probes in image-guided therapy, allowing for the visualization of tumors in early stages of the disease, effective delivery of fluorescence agents, optimized treatment to reduce side effects, and diagnosis of distant and local metastases.¹⁴

In this study, we developed hyaluronic acid (HA)-conjugated poly(lactic-co-glycolic acid) (PLGA) nanoparticles incorporating ICG (HINPs) to target cervical cancer cell lines for NIR fluorescence in vivo imaging (Fig. 1). We compared the endocytosis of HINPs and their in vitro cytotoxicity between two cell lines: CD44-positive cervical cancer cells (SiHa cells) and CD44-negative cells (cck-986-sk cells) as a control. The efficiency of in vivo delivery of HINPs in cervical cancer tumors was compared with that of free ICG. Collectively, our study demonstrated that HINPs hold the potential to enhance NIR fluorescence image-guided surgery by aiding in the visualization of CD44-positive cervical cancers.

MATERIALS AND METHODS

PLGA (Resomer[®] RG 752 H, lactide: glycolide 75:25, Mw 4000–15000), polyethylenimine (PEI, branched, Mw ~25,000), dichloromethane (DCM), dimethyl sulfoxide (DMSO), methanol, N,N'-dicyclohexylcarbodiimide (DCC), and N-hydroxysuccinimide (NHS) were purchased from Sigma-Aldrich (St. Louis, MS, USA). ICG was purchased from AdooQ (Irvine, CA, USA). Sodium hyaluronate was obtained from Lifecore Biomedical (Chaska, MN, USA). 4-(4,6-Dimethoxy-1,3,5-triazin-2-yl)-4-methylmorpholinium chloride n-hydrate (DMT-MM) was purchased from Wako Pure Chemical Industries Ltd. (Tokyo, Japan). For cell culture, Dulbecco's modified Eagle's medium (DMEM, Gibco, Grand Island, NY, USA) and Iscove's modified Dulbecco's medium (IMDM, Gibco) supplemented with 10% (v/v) fetal bovine serum (FBS) and 1% antibiotic-antimycotic solution were used. DMEM, IMDM, FBS, and phosphate-buffered saline (PBS) were purchased from Lonza Walkersville (Basel, Switzerland). The cell counting kit-8 (CCK-8) was purchased from Dojindo Laboratories Co., Ltd. (Kumamoto, Japan). All reagents used were of analytical grade.

Preparation of the HA-PLGA-ICG polymer

Co-polymer synthesis

PLGA was conjugated to PEI via the formation of an amide bond in the presence of DCC and NHS. The mixture was prepared with PLGA (200 mg) dissolved in DMSO solution (1.0 mL) by adding PEI (31 mg), DCC (16 mg), and NHS (6 mg) in

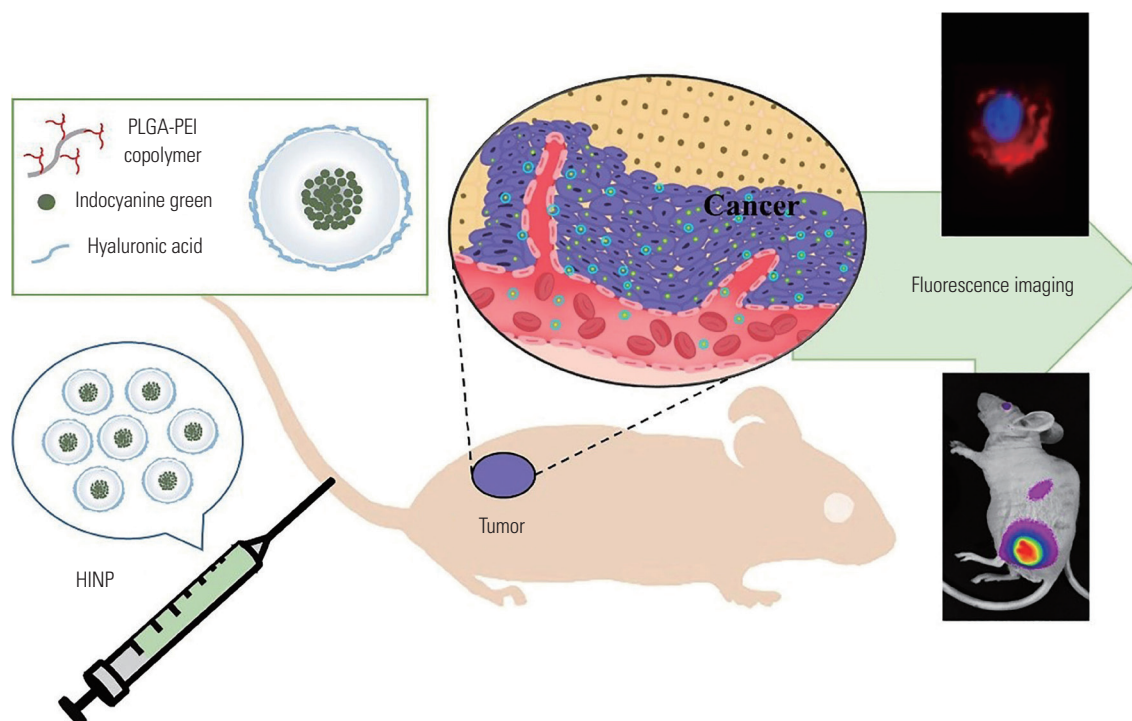


Fig. 1. Schematic illustration of ICG-loaded HA-conjugated PLGA nanoparticles (HINP) for diagnosis of cancer. ICG, indocyanine green; HA, hyaluronic acid; PLGA, poly(lactic-co-glycolic acid); PEI, polyethylenimine.

DMSO (1.5 mL) solution and stirred for 24 h at room temperature (25°C). After 24 h, the mixture was dialyzed with distilled water (DW) using a dialysis membrane (Pre-wetted RC Tubing 132576, Spectrum Laboratories, Inc., Rancho Dominguez, CA, USA) for 24 h at room temperature (25°C). After dialysis, in order to obtain the PLGA-PEI polymer, the dialyzed mixture was cryopreserved in a freeze dryer (FD-1000, Eyela, Tokyo, Japan) at -50°C, 9–10 atm for 24 h. Amide-functionalized PLGA (PLGA-NH₂) was obtained after these reactions.

Formulation of ICG-loaded PEI-PLGA polymer

The conventional oil-in-water (O/W) emulsion-solvent evaporation method was used for the formulation of ICG-loaded PLGA-NH₂ nanoparticles. The PLGA-NH₂ polymer (40 mg) was dissolved in DCM (1.0 mL), and ICG (2 mg) was dissolved in methanol (0.5 mL). The PLGA-NH₂/DCM and ICG/methanol solutions were emulsified in DW (3.0 mL) in a vial through a syringe. The obtained mixture was vortexed for 5 min and sonicated with an ultrasonic processor (VCX 130, Sonics & Materials, Newtown, CT, USA) (pulse on: 10 s, pulse off: 2 s, amplitude 80%) in a cup with ice, which prevented polymer damage caused by heat generated from the sonicator. After adding DW (9.0 mL), the solvent was evaporated with a rotary evaporator (N-1210, Eyela, Japan) for 10 min to separate the organic solvent through vacuum distillation. The distilled solvent was centrifuged at 9000 rpm for 5 min. Using the supernatant from the previous procedure, ICG-loaded nanoparticles were obtained by centrifugation at 13500 rpm for 10 min in a pro-microcentrifuge (WiseSpin CF-10, Daihan Scientific Co. Ltd., Wonju, Korea). After this reaction, the PLGA-NH₂@ICG nanoparticles were obtained.

Preparation of ICG-loaded HA-PEI-PLGA polymer

ICG-loaded HA-PEI-PLGA nanoparticles were prepared via electrostatic interactions. Briefly, dissolved ICG@PLGA-NH₂ nanoparticles in DW (1.0 mL) were added to 2.0 mL of DW containing 0.5 mL HA solution (0.5 mg/mL HA in DW) and 0.5 mL DMT-MM solution (2 mg/mL in DW). The mixture was stirred for 3 h, followed by centrifugation at 10000 rpm for 5 min.

Characterization of the nanoparticles

Measurement of particle size, zeta-potential, and stability

Particle size and zeta potential were measured using Zetasizer Nano-zs90 (Malvern Instruments Ltd., Malvern, UK). Particle morphology was characterized via transmission electron microscopy (TEM; JEOL-F200, JEOL Ltd., Tokyo, Japan). For TEM analysis, a drop of the sample solution, dissolved in DW (1 µg/mL), was placed on a 200-mesh copper grid coated with carbon and air-dried prior to measurement. The particle size distribution and zeta-potential of nanoparticles, suspended in DW (1 mg/mL), were measured using Zetasizer Nano-zs90. To further evaluate their stability, 1 mg of HINPs was dispersed in PBS at different pH levels, controlled with HCl and NaOH,

ranging from 5.0 to 8.0. The sizes of particles were monitored for 24 h using a Zetasizer Nano-zs90.

Optical properties of HINPs

The fluorescence spectra and NIR optical imaging properties of free ICG and HINPs dissolved in DMSO (1.0 mL) were measured using a Synergy HTX multi-mode reader (BioTek Instruments, Inc., Winooski, VT, USA) and the fluorescence in vivo imaging system FOBI with the NEO image software (Cellgen-tek, Cheongju, Korea), respectively.

In vitro experiments

Cell culture

SiHa cells (human cervical cancer cells) were purchased from ATCC, and ccd986sk cells (human dermal fibroblast cells) were obtained from the Korean Cell Line Bank. SiHa cells and ccd986sk cells were cultured as a monolayer in DMEM and IMDM, respectively, supplemented with 10% FBS and 1% penicillin, in a humidified incubator with 5% CO₂ at 37°C. The medium was changed every 2 days.

In vitro cytotoxicity, intracellular uptake, and blocking experiments

To test the in vitro cytotoxicity of the prepared nanoparticles, SiHa cells and ccd986sk cells (5×10³ cells/well) were seeded in 96-well plates and allowed to adhere for 24 h. After the spent medium was discarded, fresh culture medium with different concentrations of nanoparticles (1.0, 0.5, 0.25, 0.125, 0.06 mg/mL) was added to the cells, followed by incubation for 24 h under light-protected conditions. Medium without nanoparticles was used as a control. CCK-8 assay solution (10.0 µL) was added to each well, followed by incubation for 2 h at 37°C. Cytotoxicity was evaluated by measuring optical density using a Synergy HTX multimode plate reader at 450 nm. To test the in vitro cellular uptake of HINPs, SiHa cells and ccd986sk cells (5×10⁴ cells/well) were seeded in confocal dishes. The spent medium was replaced with fresh medium (2.0 mL) containing HINPs (0.5 mg/mL). The cells were incubated for 6 h and 24 h, respectively. For blocking experiments, SiHa cells and ccd986sk cells (5×10⁴ cells/well) were seeded in a confocal dish and allowed to adhere. The spent medium was replaced with fresh medium (2.0 mL) containing HA (5 µg/mL), followed by incubation for 2 h. After the addition of HINPs, the cells were incubated for 6 h and 24 h, respectively. After treatment, the cells were washed with PBS and fixed with formaldehyde solution for 30 min, followed by washing with PBS. The cells were then incubated with DAPI solution (2.0 mL, 500 nM) for 24 h at 37°C. The results of intracellular uptake and blocking experiments were observed using a Nikon Eclipse Ti fluorescence microscope (Nikon Instruments Inc., Tokyo, Japan) with NIS-Elements imaging software. Fluorescence intensity of the cells was determined to compare the intracellular uptake of HINPs in each group.

In vivo experiments

Cervical cancer xenograft model

Male BALB/c nude mice, aged 4 weeks, were obtained from

Junbiotech Inc. (Suwon, Korea) and kept under standard conditions with air filtration. To establish the animal cervical tumor model, SiHa cells (5×10^6 cells/mL/mouse) were subcutaneously injected into the left flank of the nude mice, as reported

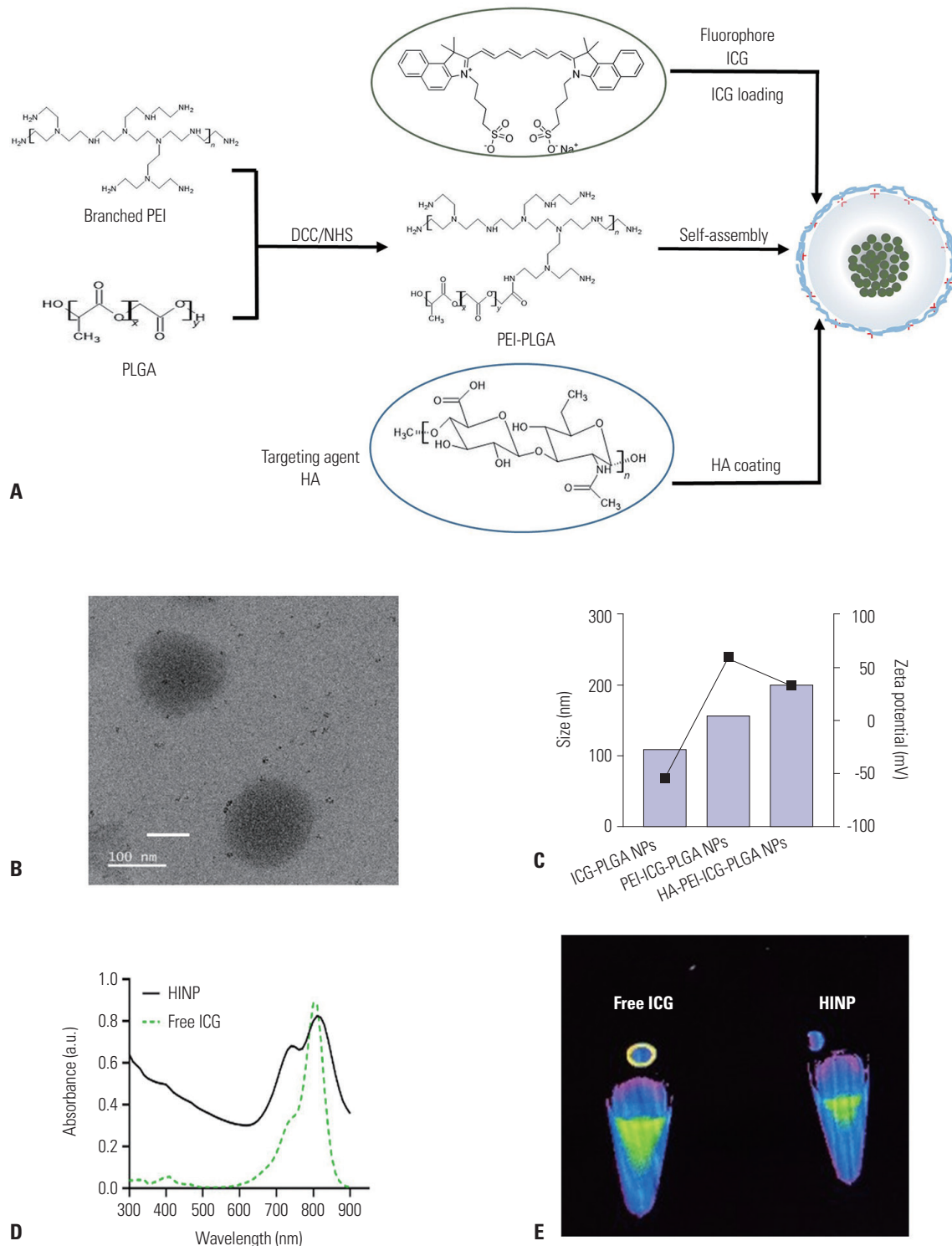


Fig. 2. Synthesis and Characterization of nanoparticles. (A) Structural formula of the ICG-loaded HA-conjugated PLGA nanoparticles (HINPs). (B) Transmission electron microscopy image of HINP and (C) comparison of size and zeta-potential via dynamic light scattering. (D) Spectral absorbance and (E) near-infrared images of free ICG and the HINPs. ICG, indocyanine green; HA, hyaluronic acid; PLGA, poly(lactic-co-glycolic acid); PEI, polyethylenimine; DCC, dicyclohexylcarbodiimide; NHS, N-hydroxysuccinimide.

previously.¹⁵ All animal housing and experimental procedures were reviewed and approved by the Institutional Animal Care and Use Committee of Yonsei University at Wonju (YWCI-202105-008-04). All experiments were carried out in accordance with the relevant guidelines and regulations established by the Institutional Animal Care and Use Committee of Yonsei University at Wonju and the Institutional Biosafety Committee of Yonsei University at Wonju.

Biodistribution of nanoparticles

Tumors were allowed to grow on the mice for 4 weeks until they were 1–1.5 cm in size. Then, the tail veins of mice were injected with free ICG (N=3, 0.01 mg/0.1 mL/mouse) or HINPs (N=3, 0.1 mg/0.1 mL/mouse); the mice were sacrificed 24 h after injection. Different organs, such as the lungs, liver, spleen, heart,

kidneys, and tumors, were collected, and fluorescence images of these organs were obtained using an FOBI in vivo imaging system equipped with the NEO software (Cellgentek). Fluorescence intensity was measured using ImageJ software (National Institutes of Health, Bethesda, MD, USA).

Statistics

The data were expressed as mean±standard deviation and comparisons were performed using one-way ANOVA tests (Systat Software, Inc., Chicago, IL, USA). Differences were considered statistically significantly at * $p<0.05$, ** $p<0.01$, *** $p<0.005$, and **** $p<0.001$.

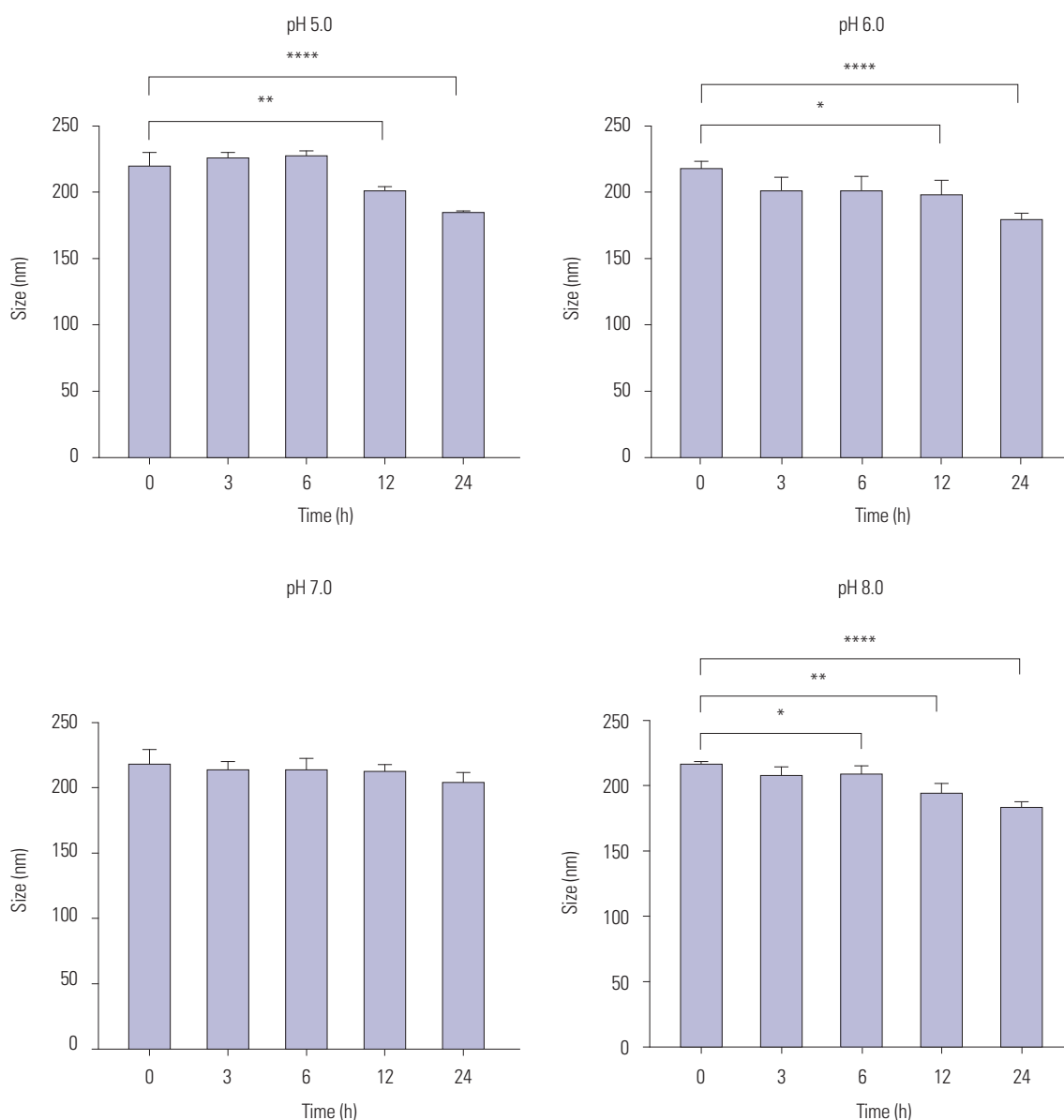


Fig. 3. Stability of ICG-loaded HA-conjugated PLGA nanoparticles (HINPs) in various pH conditions in the range of 5.0–8.0. * $p<0.05$, ** $p<0.01$, **** $p<0.001$. ICG, indocyanine green; HA, hyaluronic acid; PLGA, poly(lactic-co-glycolic acid).

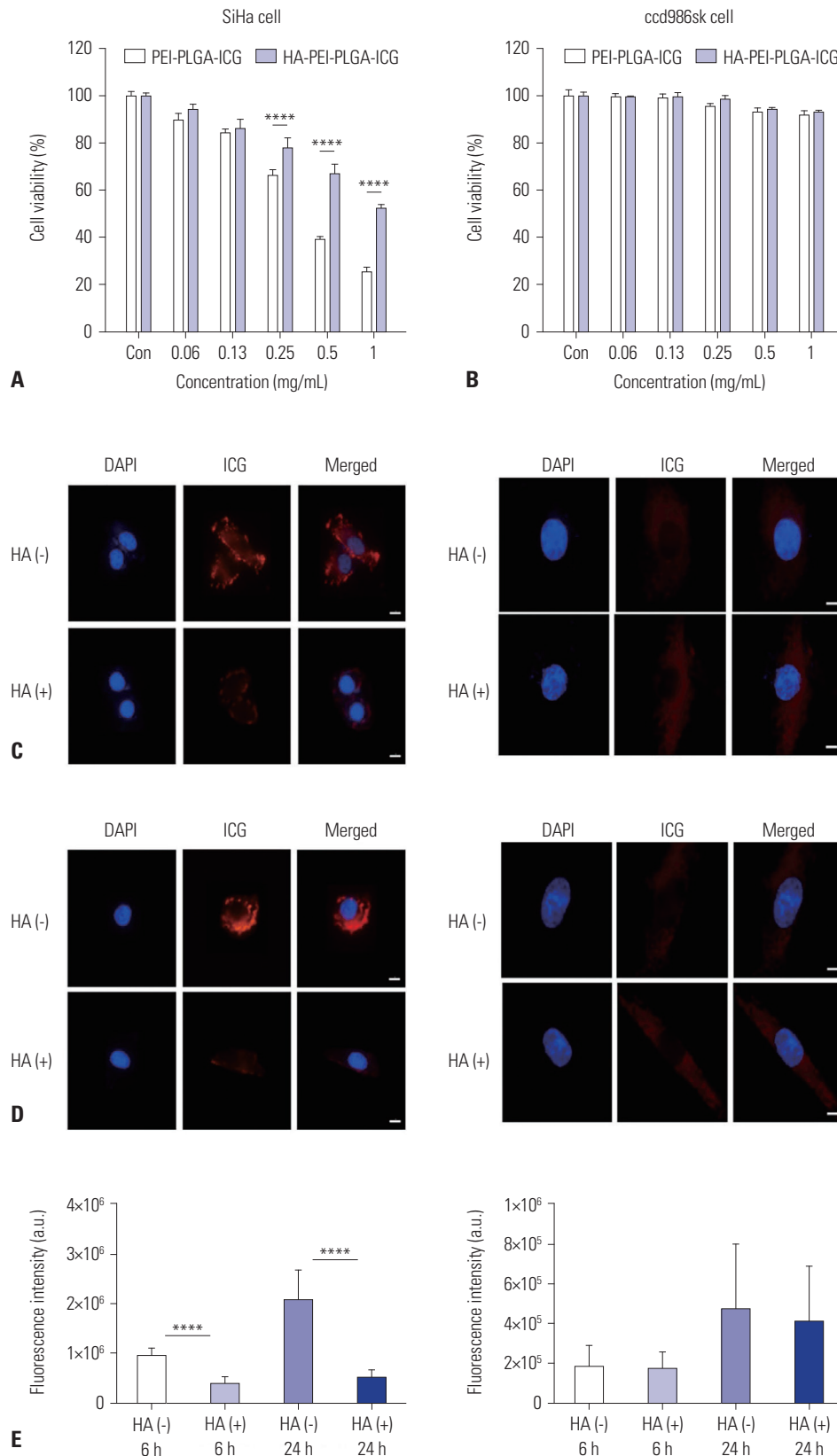


Fig. 4. Comparison of nanoparticle cytotoxicity in CD44-positive cervical cancer cells (A: SiHa cells) and human dermal fibroblast cells (B: ccd986sk cells). Comparison of intracellular uptake post-injection at (C) 6 h and (D) 24 h. (E) Quantitative average fluorescence intensities in SiHa and ccd986sk cells treated with or without free HA (scale bar: 10 μ m, HA +: pretreated cells with HA, HA -: cells without treatment). **** p <0.001. ICG, indocyanine green; HA, hyaluronic acid; PLGA, poly(lactic-co-glycolic acid); PEI, polyethylenimine.

RESULTS

Preparation and characterization of HINPs

HINPs were prepared via O/W emulsion with ICG and then coated with HA on PLGA-conjugated PEI. First, the PEI-PLGA co-polymer was synthesized via an amide coupling reaction with the NHS-DCC reagent. Second, PEI-PLGA nanoparticles, encapsulated with ICG, were formed via the emulsion method using PEI-PLGA and ICG. Finally, HINPs were synthesized through chemical coupling between the carboxylic groups in HA and the amine groups on the surface of PEI-PLGA nanoparticles. This process is depicted in Fig. 2A. TEM images revealed that the HINPs had a well-defined spherical shape (Fig. 2B). The average diameter and zeta-potential of the HINPs, as observed via dynamic light scattering analysis, were 200.0 ± 48.83 nm and 32.9 ± 5.67 mV, respectively. UV-Vis fluorescence spectra were also obtained to confirm the presence of HINPs. HINPs showed ICG fluorescence signals upon excitation with a 780 nm laser, which was consistent with the fluorescence spectra of ICG. Free ICG and HINPs showed similar fluorescence intensities in NIR images (Fig. 2C and D). The stability of the nanoparticles was determined through the degree of degradation, as evidenced by changes in size over time at different pH ranges (5.0–8.0). The HINPs showed no significant size

change in solutions with pH values of 5.0 to 8.0 for 12 h; however, a size change was observed in the particles at pH 7.0 after 12 h (Fig. 3).

Cellular uptake and cytotoxicity of HINPs

SiHa cells (CD44-positive cervical cancer cells) were selected to confirm the responses of the nanoparticles against cervical cancer, and ccd986sk cells (CD44-negative human skin fibroblast cells) were selected to confirm the responses of the nanoparticles against normal cells. Experiments with these cells assessed the cytotoxicity of nanoparticles and differences in cellular uptake depending on endocytosis with or without CD44-HA binding. Cytotoxicity experiments confirmed the viability of the cells after treatment with different types of nanoparticles at various concentrations. The viability of both types of cells that received treatment with HINPs coated with HA was significantly increased, compared to that of cells treated with cationic polymers ($p < 0.001$) at a concentration of more than 0.25 mg/mL (Fig. 4A and B).

To confirm differences in cellular uptake depending on endocytosis with or without CD44-HA binding, both cells pretreated with HA and those without any treatment were prepared. In cells that had been pretreated with HA, CD44 receptor function is inhibited in response to HA present on HINPs. The

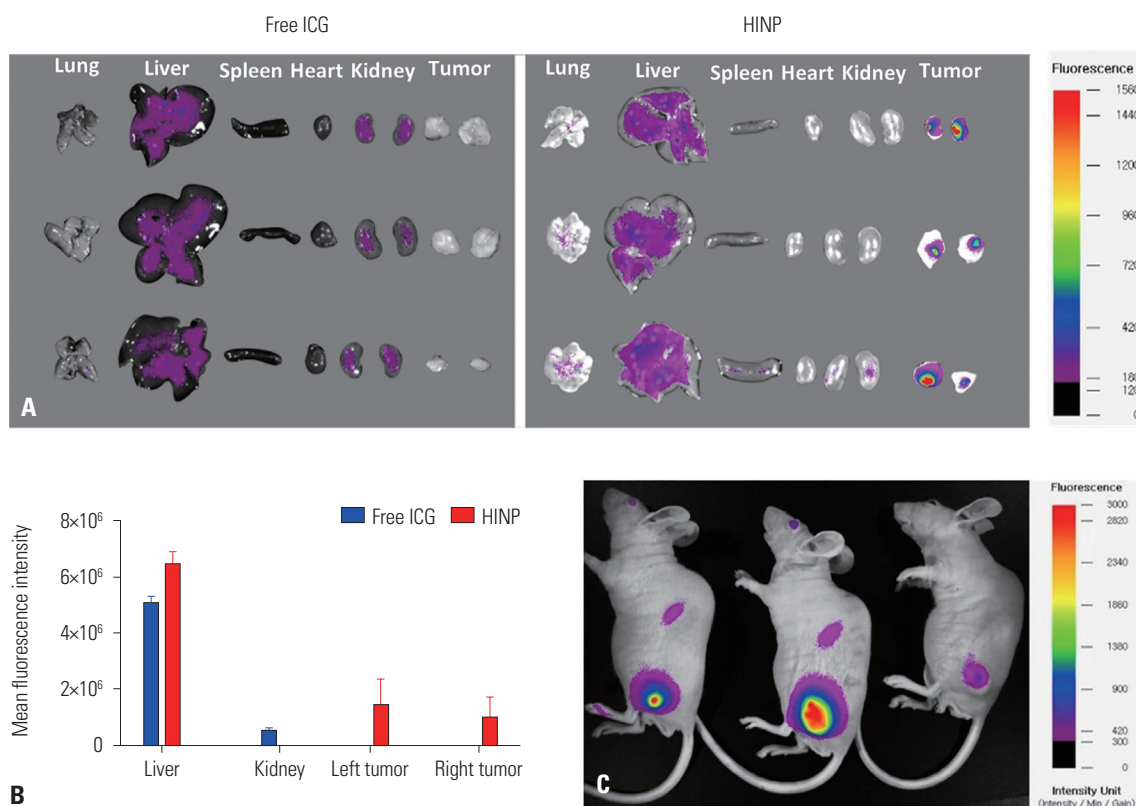


Fig. 5. In vivo fluorescence imaging of ICG-loaded HA-conjugated PLGA nanoparticles (HINPs), compared with free ICG, after the systemic delivery of nanoparticles through intravenous injection. (A) Fluorescence imaging of different organs 24 h post-injection with HINPs or free ICG. (B) Quantitative average fluorescence intensities of the biodistribution of the particles in different organs and in the tumors. (C) Near infra-red imaging of nude mice. ICG, indocyanine green; HA, hyaluronic acid; PLGA, poly(lactic-co-glycolic acid).

HA-preprocessed cells were marked as HA+, and unprocessed cells were marked as HA-. After HINP treatment of each cell, 6-h and 24-h fluorescence images and fluorescence intensity were compared. The fluorescence images shown in Fig. 4 demonstrate that the cells treated with HINPs exhibited dispersed red fluorescence in the cytoplasm due to ICG. This means that the ICG-encapsulated HINPs were successfully internalized by CD44-positive cervical cells and CD44-negative cells. When CD44-positive cervical cancer cells were incubated with free HA as a CD44-specific ligand following treatment with HINPs, the fluorescence intensities decreased significantly ($p < 0.001$), compared to untreated cells, while the fluorescence intensities of CD44-negative cells were not significantly different between HA-treated cells and untreated cells (Fig. 4).

Preparation of a xenograft model and biodistribution studies

A cervical cancer model was constructed using nude mice. SiHa cells were subcutaneously injected into the left flank of these mice to form tumors. After the tumors grew to a size range of 1–1.5 cm, HINPs were injected into the tail vein, and the mice were sacrificed 24 h post-injection. Fluorescence images of the tumors and major organs were obtained to visualize the biodistribution of free ICG and HINPs. After injecting free ICG, most of it accumulated in the liver at 24 h, followed by the kidneys and the lungs. Apparently, the HINPs increased the accumulation of ICG in the tumors, followed by that in the liver. Fluorescence analysis showed that the mean fluorescence intensity of HINPs in the tumor was much higher than that of free ICG, which had little intensity (Fig. 5).

DISCUSSION

The development of nano-drug delivery systems using nanoparticles have recently received considerable attention. Polymeric nanoparticles are a common form of nanocarriers used in drug delivery applications that can be synthesized by combining multiple functional units with other molecules or via co-polymer self-assembly. PLGA, an FDA-approved polymeric carrier with biodegradable and biocompatible properties, has been used in therapeutic applications of ICG. Compared to free ICG, nanoparticles containing PLGA compensate for the limitations of ICG by improving its stability in light, extreme temperatures, and certain solvents, as well as extending its half-life in the body.^{16–19}

The development of contrast agents that specifically bind to lesions could facilitate the rapid development of molecular imaging techniques. Recent studies have reported methods of bio-conjugating multiple molecular moieties to ICG to create imaging probes that can bind specifically to cancer tissues and allow normal tissue and cancer tissue to be distinguished in real-time during surgery.²⁰ CD44, which plays a role in cell pro-

liferation and invasion, is involved in the activity of cancer cells, and is expressed in various types of cancer cells. HA, which has biodegradable, biocompatible, non-toxic, and non-immunogenic properties, is the primary ligand of CD44 receptor. Ligand-receptor reactions between HA and CD44 receptor could improve the target-specificity of particles for applications facilitated through receptor-mediated endocytosis.^{21–23}

Some studies have used PLGA and targeting agents that show screening and therapeutic effects through NIRF imaging. Xin, et al.²⁴ synthesized new nanoparticles by combining the fluorescent agent ICG with the antioxidant resveratrol and the target agent folic acid. These new particles were tested in vitro and in vivo using U87 glioma cells. Park, et al.²⁵ reported a molecular imaging technique that combined pH-sensitive poly (β -amino ester), HA, and ICG to synthesize new nanoparticles/nano-gels that respond to different pH levels to detect and identify cancer cells in in vitro experiments using breast cancer cell lines. Hill, et al.²⁰ successfully performed an in vivo study using a synthesized nanoparticle that combined HA and ICG, and observed breast cancer tissue with NIR fluorescence images in mice implanted with xenografts to differentiate cancer tissue from normal tissue in real-time. Nanoparticles that compensate for the shortcomings of ICG have opened up the possibility of applying image-guided surgical techniques by checking the margins of tumors. However, no studies have reported on the application of nanoparticles binding ICG and HA in cervical cancer.

In this study, we developed HINPs designed as a polymeric vehicle of ICG with a targeting function, and demonstrated that these particles were more effective in cervical cancer cell targeting and stable visualization by overcoming the limitations of ICG. In the conjugation of agents to construct HINPs, the components of HINPs were identified through changes in zeta potential and increases in size. Dynamic light scattering data revealed changes in the size and zeta potential of the nanoparticles, which was also observed in previous stages, confirming the binding between carboxylic and amine groups. As PLGA has a carboxyl group at its terminal end, the zeta potential of the ICG-loaded PLGA nanoparticles was -54.6 mV, indicating a negative charge. As PEI has abundant amine groups, the surface potential of ICG-loaded nanoparticles containing PEI-PLGA was 60.4 mV, showing that the surface potential changed to a positive charge. Due to the presence of HA coating on the surface of the nanoparticles, the surface potential of HINPs was 32.9 mV, a less positive value, compared to that of the PEI-ICG-PLGA nanoparticles. Bonds between substances and materials can be indirectly identified through changes in their zeta potential. In addition, HINP had similar fluorescence intensities in the NIR fluorescent images with ICG. These results reveal that ICG maintains its optical properties even under particulate conditions (Fig. 2).

HINPs had an average diameter of 200 nm and showed a clear accumulation in cervical cancer tumors. This result could

be explained by the enhanced permeability and retention effect, which is effective for nano-sized particles in the range of 100–400 nm.²⁶ HINPs showed good stability, with no significant size differences upon subjection to neutral and acidic conditions within 12 h (Fig. 3). This can be useful to maintain the characteristics of HINPs not only in blood circulation but also in acidic conditions of the tumor microenvironment.²⁷

PEI has also been reported to induce cell dysfunction.²⁸ In this study, the cytotoxicity caused by PEI was higher in CD44-positive cervical cancer cells (SiHa cells) than in CD44-negative cells (ccd986sk cells), and the cytotoxicity by HINPs was significantly lower than that of cationic polymers ($p < 0.001$), with a concentration of nanoparticles at more than 0.25 mg/mL. In CD44-positive cervical cancer cells, the cell group without any HA treatment before the addition of HINPs (HA-) had much higher cellular uptake of HINPs than the cell group that was pretreated with HA before the addition of HINPs (HA+). These significant differences in CD44-positive cells with and without HA pretreatment showed that the pretreated HA coupled to CD44 receptors on the CD44-positive cancer cells and may have blocked coupling between the CD44 receptors and HINPs.²⁹ A comparison of the fluorescence results at 6 h and 24 h showed that the nanoparticles accumulated in cells over time for up to 24 h (Fig. 4C and D). The intracellular uptake of nanoparticles indicates that HINPs target CD44-positive cervical cancer cells specifically through receptor-mediated endocytosis (Fig. 4). Statistically significant differences between CD44-positive cervical cancer models injected with HINPs and those injected with free ICG were observed upon fluorescence intensity analysis of the tumors at 24 h after injection. Observation at 24 h after injection was performed because we found sufficient accumulation at 24 h with preliminary experiments, due to the properties of HINPs, including long circulation and active targeting (not shown).

When comparing the biodistribution of free ICG to that of HINPs, mean fluorescence intensities in the major organs and tumors of the HINP-treated mice were higher than those in the free ICG-treated mice, which is consistent with previously reported results.¹⁶ This is likely because ICG has a short half-life and is known to be mostly discharged through the liver due to hepatic clearance, along with the fact that HINPs remained stable for up to 24 h in solutions of neutral pH.¹⁶ In tumor models injected with HINPs, the accumulation of HINPs was higher in larger tumors. This could be explained by the increased angiogenesis in larger tumors, representing more CD44 receptors from both cancer cells and new blood vessels. Thus, passive targeting through particle size selection and active targeting via the presence of HA from the HINPs can be more effective than free ICG in visualizing cervical cancer cells (Fig. 5).

In conclusion, this study showed that HINPs with CD44-targeting capability are suitable nanocarriers with which to deliver ICG and can be used for visualizing CD44-positive cervical cancer cells and angiogenesis. The HINPs synthesized in this

study enhance the stability of ICG and exhibit cytotoxic effects and intracellular uptake through CD44 receptor-mediated endocytosis in cervical cancer cells, both in vitro and in vivo. With further clinical research, we expect that HINPs will be proven to increase the effectiveness of ICG. Therefore, HINPs could be a promising multifunctional diagnostic and screening platform in image-guided surgery for cervical cancer and promote significant advances in the field of gynecologic oncology.

ACKNOWLEDGEMENTS

This research was partially funded by grant numbers 2018R1D1A1B07042339, 2019K2A9A2A08000123, and Leaders in Industry-university Cooperation+Project supported by the Ministry of Education and National Research Foundation of Korea.

AUTHOR CONTRIBUTIONS

Conceptualization: Jaehong Key and San-Hui Lee. **Data curation:** Seonmin Choi, Sanghyo Park, and Chaewon Park. **Formal analysis:** Sanghyo Park and Chaewon Park. **Funding acquisition:** Jaehong Key. **Investigation:** Seonmin Choi, San-Hui Lee, Sanghyo Park, and Sun Hwa Park. **Methodology:** Seonmin Choi and Sanghyo Park. **Project administration:** Jaehong Key. **Resources:** Jaehong Key. **Supervision:** Jaehong Key. **Validation:** Seonmin Choi, San-Hui Lee, and Jaehong Key. **Writing—original draft:** Seonmin Choi and San-Hui Lee. **Writing—review & editing:** Jaehong Key. **Approval of final manuscript:** all authors.

ORCID iDs

Seonmin Choi	https://orcid.org/0000-0002-6716-6422
San-Hui Lee	https://orcid.org/0000-0002-5041-4741
Sanghyo Park	https://orcid.org/0000-0002-2730-1001
Sun Hwa Park	https://orcid.org/0000-0002-9006-5427
Chaewon Park	https://orcid.org/0000-0002-8886-9995
Jaehong Key	https://orcid.org/0000-0002-3453-2123

REFERENCES

1. Sung H, Ferlay J, Siegel RL, Laversanne M, Soerjomataram I, Jemal A, et al. Global cancer statistics 2020: GLOBOCAN estimates of incidence and mortality worldwide for 36 cancers in 185 countries. *CA Cancer J Clin* 2021;71:209-49.
2. Ferlay J, Colombet M, Soerjomataram I, Mathers C, Parkin DM, Piñeros M, et al. Estimating the global cancer incidence and mortality in 2018: GLOBOCAN sources and methods. *Int J Cancer* 2019;144:1941-53.
3. Li B, Xia X, Chen J, Xia D, Xu R, Zou X, et al. Paclitaxel-loaded lignin particle encapsulated into electrospun PVA/PVP composite nanofiber for effective cervical cancer cell inhibition. *Nanotechnology* 2021;32:015101.
4. Janicek MF, Averette HE. Cervical cancer: prevention, diagnosis, and therapeutics. *CA Cancer J Clin* 2001;51:92-114.
5. Gioux S, Choi HS, Frangioni JV. Image-guided surgery using invisible near-infrared light: fundamentals of clinical translation. *Mol Imaging* 2010;9:237-55.

6. Lee BT, Hutteman M, Gioux S, Stockdale A, Lin SJ, Ngo LH, et al. The FLARE intraoperative near-infrared fluorescence imaging system: a first-in-human clinical trial in perforator flap breast reconstruction. *Plast Reconstr Surg* 2010;126:1472-81.
7. Buda A, Passoni P, Corrado G, Bussi B, Cutillo G, Magni S, et al. Near-infrared fluorescence-guided sentinel node mapping of the ovary with indocyanine green in a minimally invasive setting: a feasible study. *J Minim Invasive Gynecol* 2017;24:165-70.
8. Holloway RW, Bravo RA, Rakowski JA, James JA, Jeppson CN, Ingersoll SB, et al. Detection of sentinel lymph nodes in patients with endometrial cancer undergoing robotic-assisted staging: a comparison of colorimetric and fluorescence imaging. *Gynecol Oncol* 2012;126:25-9.
9. West W, Pearce S. The dimeric state of cyanine dyes. *J Phys Chem* 1965;69:1894-903.
10. Zhou JF, Chin MP, Schafer SA. Aggregation and degradation of indocyanine green. In: Anderson RR, editor. *Laser surgery: advanced characterization, therapeutics and systems IV*. Bellingham, WA: SPIE; 1994. p.495-505.
11. van den Biesen PR, Jongsma FH, Tangelder GJ, Slaaf DW. Yield of fluorescence from indocyanine green in plasma and flowing blood. *Ann Biomed Eng* 1995;23:475-81.
12. Desmettre T, Devoisselle JM, Mordon S. Fluorescence properties and metabolic features of indocyanine green (ICG) as related to angiography. *Surv Ophthalmol* 2000;45:15-27.
13. Li Y, Wen T, Zhao R, Liu X, Ji T, Wang H, et al. Localized electric field of plasmonic nanoplatform enhanced photodynamic tumor therapy. *ACS Nano* 2014;8:11529-42.
14. Wang H, Li X, Tse BW, Yang H, Thorling CA, Liu Y, et al. Indocyanine green-incorporating nanoparticles for cancer theranostics. *Theranostics* 2018;8:1227-42.
15. Hsiao YH, Hsieh MJ, Yang SF, Chen SP, Tsai WC, Chen PN. Phloretin suppresses metastasis by targeting protease and inhibits cancer stemness and angiogenesis in human cervical cancer cells. *Phytomedicine* 2019;62:152964.
16. Wiegand BD, Ketterer SG, Rapaport E. The use of indocyanine green for the evaluation of hepatic function and blood flow in man. *Am J Digest Dis* 1960;5:427-36.
17. Manchanda R, Fernandez-Fernandez A, Nagesetti A, McGoron AJ. Preparation and characterization of a polymeric (PLGA) nanoparticulate drug delivery system with simultaneous incorporation of chemotherapeutic and thermo-optical agents. *Colloids Surf B Biointerfaces* 2010;75:260-7.
18. Bahmani B, Gupta S, Upadhyayula S, Vullev VI, Anvari B. Effect of polyethylene glycol coatings on uptake of indocyanine green loaded nanocapsules by human spleen macrophages in vitro. *J Biomed Opt* 2011;16:051303.
19. Saxena V, Sadoqi M, Shao J. Polymeric nanoparticulate delivery system for Indocyanine green: biodistribution in healthy mice. *Int J Pharm* 2006;308:200-4.
20. Hill TK, Abdulahad A, Kelkar SS, Marini FC, Long TE, Provenzale JM, et al. Indocyanine green-loaded nanoparticles for image-guided tumor surgery. *Bioconjug Chem* 2015;26:294-303.
21. Chen C, Zhao S, Karnad A, Freeman JW. The biology and role of CD44 in cancer progression: therapeutic implications. *J Hematol Oncol* 2018;11:64.
22. Tran TH, Choi JY, Ramasamy T, Truong DH, Nguyen CN, Choi HG, et al. Hyaluronic acid-coated solid lipid nanoparticles for targeted delivery of vorinostat to CD44 overexpressing cancer cells. *Carbohydr Polym* 2014;114:407-15.
23. Yan HM, Song J, Jia X, Zhang Z. Hyaluronic acid-modified didecyldimethylammonium bromide/d- α -tocopheryl polyethylene glycol succinate mixed micelles for delivery of baohuoside I against non-small cell lung cancer: in vitro and in vivo evaluation. *Drug Deliv* 2017;24:30-9.
24. Xin Y, Liu T, Yang CL. Development of PLGA-lipid nanoparticles with covalently conjugated indocyanine green as a versatile nanopatform for tumor-targeted imaging and drug delivery. *Int J Nanomed* 2016;11:5807-20.
25. Park HS, Lee JE, Cho MY, Hong JH, Cho SH, Lim YT. Hyaluronic acid/poly(β -amino ester) polymer nanogels for cancer-cell-specific NIR fluorescence switch. *Macromol Rapid Commun* 2012;33:1549-55.
26. Wilhelm S, Tavares AJ, Dai Q, Ohta S, Audet J, Dvorak HF, et al. Analysis of nanoparticle delivery to tumours. *Nat Rev Mater* 2016;1:16014.
27. Wojtkowiak JW, Verduzco D, Schramm KJ, Gillies RJ. Drug resistance and cellular adaptation to tumor acidic pH microenvironment. *Mol Pharm* 2011;8:2032-8.
28. Moghimi SM, Symonds P, Murray JC, Hunter AC, Debska G, Szczyk A. A two-stage poly(ethylenimine)-mediated cytotoxicity: implications for gene transfer/therapy. *Mol Ther* 2005;11:990-5.
29. Wan L, Jiao J, Cui Y, Guo J, Han N, Di D, et al. Hyaluronic acid modified mesoporous carbon nanoparticles for targeted drug delivery to CD44-overexpressing cancer cells. *Nanotechnology* 2016;27:135102.